

Tie-dye technique and pattern features

Liu Su-qiong^{1,3}, Gao Wei-dong¹, Xue Wei², Gu Ming⁴ & Liang Hui-e^{1,a}

¹ School of Textile and Garment, Jiangnan University, Wuxi, Jiangsu 214 122, China

² Department of Computer, Nanjing Agricultural University, Nanjing, Jiangsu 210 002, China

³ Art College, JinLing Institute of Technology, Nanjing, Jiangsu 211 169, China

⁴ Jiangsu Huayi Group, Haian, Jiangsu 226 600, China

Received 6 June 2014; revised received and accepted 26 August 2014

Relationship between tie-dye technique and image pattern has been studied. Based on digital image processing, average value of HSV (hue, saturation, value) tri-component of valid tie-dye area, proportion of incompletely dyed area in HSV color space and the Tamura first three texture features of digital tie-dye image have been extracted. Then, the repeated tests and analysis of variance (ANOVA) of rotation speed and concentration have been done. The results show the obvious impact of concentration and rotation speed on the color and texture feature of tie-dye pattern. Furthermore, back propagation neural network is developed and partial pattern features with low correlation is used to forecast the tie-dye concentration and rotation speed. The experiment results show the 100% rate of forecast, which proves that pattern features can effectively achieve the technique forecast.

Keywords: Digital image processing, Neural network, Tie-dye technique

1 Introduction

The tie-dye technique has specificity on production management, technical process and effect evaluation. When the enterprises obtain the sample order, the technicians should firstly analyze the color and texture of sample, then design the corresponding production technical parameters according to their experience and arrange the trial production of sample order. Because of flexibility of techniques and the different understanding of the technicians over the pattern, the technicians might produce different technical parameters for the same sample. The subjective decision leads to the dependence of tie-dye businesses on human experiences, extensive management, low sample precision and slow response speed. So, we built a model to forecast the tie-dye technique by our proposed features of digital tie-dye image.

To evaluate the tie-dye pattern, the human subjective assessment is based on the color and texture. So, with computer image technique, objective quantitative evaluation of tie-dye pattern can be based on such evaluation habits to quantify color shade, white space (incompletely dyed area) and texture.

Color is an important visual feature of the image. So, the method of using color to identify image has been widely applied. The extraction of color information should use proper color space. There are a lot of applications of extracting characteristics from color space for relevant analysis within the field of face recognition, remote sensing analysis and traffic management.

Xiaohua *et al.*¹ adopt Gabor transition to extract Gabor feature from the RGB color images (red, green, blue) component and use for image classification. Keke *et al.*² take $(S+V)/H$ value to characterize the skin color, which could enhance the recognition capacity of HSV space upon the skin of human. HSU *et al.*³ establish the relationship between model of YCrCb color space and skin color. Amine *et al.*⁴ sum up the Gaussian distribution in the pure-color space YCrCb to classify the pixels. Wei and De-ren⁵ introduce the hue component of HSV color space to the cloud test system. Martel-Brisson and Zaccarin⁶ develop the method to cut the shadow of moving vehicle on the edge of HSV color space. Cucchiara *et al.*⁷ firstly adopt the middle-value filtering to obtain the background model, then utilize the similar hue and saturation and the difference of lightness between the shadow of moving vehicles and the background pixels within HSV color space to

^a Corresponding author.
E-mail: lianghe@jiangnan.edu.cn

identify and separate the shadow of moving vehicle. Yang Hongyin *et al.*⁸ come up with an image indexing method on the basis of HSV space color edge histogram.

So, on comparing the models of RGB and YCrCb, HSV color space is found better to describe the color. HSV color space has two important features, viz *V* component is not related to color information, *H* component and *S* component are closely related to the style how the human eyes observe the colors. These features make the HSV color space suitable for digital image processing. So, it is thought to analyse tie-dye image within HSV color space.

Texture is a key component of human visual perception. It describes the homogeneity of image surface and the spatial distribution of different elements not depending on the color and brightness information. It reflects the global and local structure of images and is widely used for image retrieval. Texture methods can be categorized as statistical, geometrical, structural, model-based and signal processing features. There are many texture feature extraction methods, including wavelet-based texture feature, Tamura feature and feature gray-level co-occurrence matrix⁹. Tamura¹⁰ features have six dimensions including coarseness, contrast, directionality, line-likeness, regularity and roughness, which take into account human perception of texture. The last three components can be derived from the first three. So, the first three have been used for texture analysis in this paper.

Based on the digital image processing technology, this paper extracts the average value of HSV tri-component of the valid tie-dye area, the proportion of tie-dye white area and Tamura texture as pattern features. A set of variance experiments are designed to validate the strong relationship between the tie-dye technique and the characteristic quantity of color and texture. Then a mathematic model is built up to forecast the tie-dye technique (the tie-dye concentration, rotation speed) with the characteristic quantity of color and texture.

2 Materials and Methods

2.1 Materials

The experiments were carried out under the indoor temperature of 25°C. We selected 18.2tex 140g/m² cotton knitted fabric and cut into size of 60cm×40cm. These fabrics were then pinched and tied tightly with space of about 1cm apart. Then the

samples were soaked at 100°C for 120 min and separately put into 5 different dyeing levels (Table 1) at 60° C and 100% regain. Table 1 shows the required amount (gram) of reactive dyes and auxiliaries for 100g fabric; reactive black KN-B and reactive red B-2BF are reactive dyes, and sodium sulphate (anhydrous) (SSA) and soda ash (SA) are two auxiliaries contents in water. Auxiliaries in all 5 vats also contain 0.5g/L detergent, 0.5g/L glacial acetic acid, 1g/L anti-staining agent and 2g/L softener. Each sample was prepared with three rotation speeds, namely 5 circles/min, 15 circles/min and 30 circles/min. After dyeing, the fabrics were washed and dried. Finally, they were scanned by high-definition scanner with resolution of 300dpi. The images (27cm×42cm) were collected, and stored with RGB mode (Fig.1).

2.2 Methods

The processing of tie-dye image includes two steps, viz image preprocessing and extraction of pattern features.

Preprocessing includes the procedure of image space conversion, smooth filtering and image segmentation. The pattern information includes the average value of HSV tri-component of the valid tie-dye area, the proportion of tie-dye white area of the image and Tamura texture.

The scanned image was saved in RGB color model which produces 24-digit color space through the sensitivity quantity of sensitive components of *R*, *G*, and *B* at each pixel. The conversion formula from the RGB model to

HSV model is as follows:

$$\begin{aligned}
 H &= \begin{cases} 0 & \text{if max} = \text{min} \\ 60 \times \frac{G - B}{\text{max} - \text{min}} + 0 & \text{if max} = R \text{ and } G \geq B \\ 60 \times \frac{G - B}{\text{max} - \text{min}} + 360 & \text{if max} = R \text{ and } G < B \\ 60 \times \frac{B - R}{\text{max} - \text{min}} + 120 & \text{if max} = G \\ 60 \times \frac{R - G}{\text{max} - \text{min}} + 240 & \text{if max} = B \end{cases} \\
 S &= \begin{cases} 0 & \text{if max} = 0 \\ 1 - \frac{\text{min}}{\text{max}} & \text{else} \end{cases} \\
 V &= \text{max} \quad \dots (1)
 \end{aligned}$$

RGB color matrix has been normalized within [0, 1] with linear function, max is the maximum value and min is the minimum value among *R*, *G* and *B*. The scope of *H* value after conversion ranges from

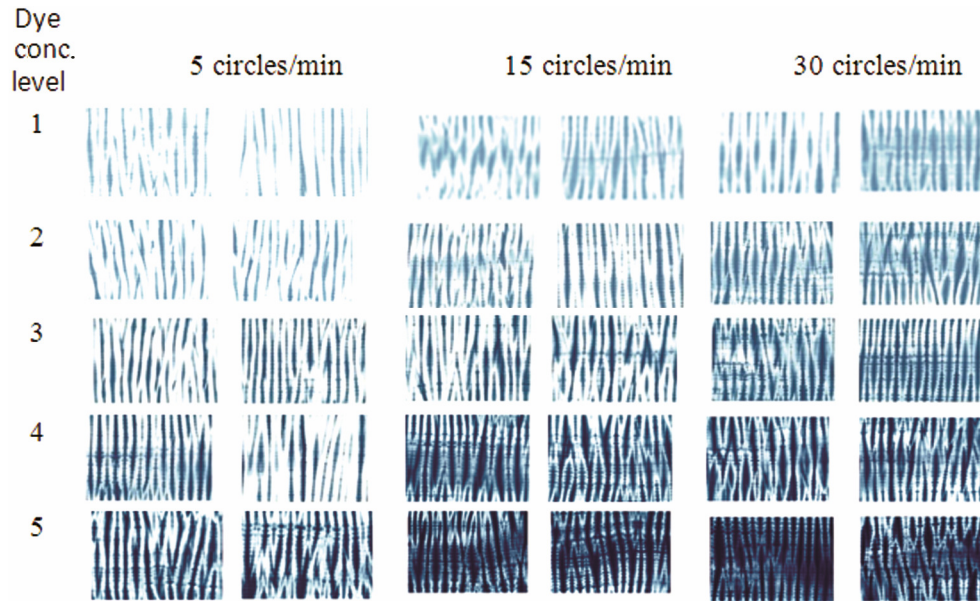


Fig. 1—Experimental samples

0 to 360, and *S* value and *V* value are in the range [0, 1]. For the subsequent treatment, *H* is normalized to the range of [0, 1] with linear function.

2.2.1 Image Processing

2.2.1.1 Noise Reduction

The tie-dye images interfere within the complex environment, so it is necessary to filter the images.

The median filter is the nonlinear digital filtering technique. It has the advantages of easy calculation and high feasibility. The filter adopts a sliding window with odd points. In each matrix of HSV, the median of every elemental value replaces the gray value of the central point. If the number of elements is odd, the value in the middle is the median. If the number of elements is even, the average value of two values in the middle is the median. This paper adopts 3×3 median filter to eliminate the noise, the filtered images become smoother (Fig.2).

2.2.1.2 Image Segmentation

The study adopts Otsu algorithm to segregate the tie-dye images into dyeing area and white area.

Assume *L* is the largest gray level in gray level image. Otsu¹¹ method describes the following criterion for selecting the optimum threshold *t*:

$$\max_t \{ w_0(t) \times [u_0(t) - u]^2 + w_1(t) \times [u_1(t) - u]^2 \} \dots (2)$$

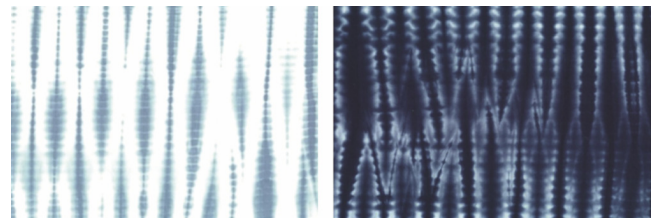


Fig. 2—Filtering effect diagram of two examples

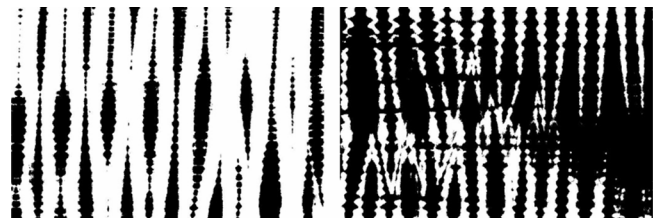


Fig. 3—Segmentation image of two examples

where *t* is the threshold, $t \in [0, L-1]$; *w*₀, the background proportion; *u*₀, the background average value; *w*₁, the foreground proportion; *u*₁, the foreground average value; and *u*, the average value of the whole image. The value *t*, which makes the expression formula above maximum, is the best threshold value of image segmentation (Fig. 3).

2.2.2 Feature Extraction

2.2.2.1 Color Feature

Color features of the image include the average value of HSV tri-component of valid tie-dye area and

proportion of white area. Calculation formula of HSV average value is defined as:

$$\begin{aligned}
 H_m &= \frac{1}{N} \sum H(i, j) \\
 S_m &= \frac{1}{N} \sum S(i, j) \\
 V_m &= \frac{1}{N} \sum V(i, j) \quad (i, j) \in W \quad \dots(3)
 \end{aligned}$$

where W is the pixel coordinate of black area in segmentation image; and N , the pixel number of that area; both of them are obtained through image segmentation.

Assuming all pixels in image as M and all image pixels in dyeing area as F , the proportion of incompletely dyed area is as follows:

$$Q = (M-F)/M \quad \dots(4)$$

2.2.2.2 Tamura Texture Feature Extraction

Coarseness

Coarseness is designed to measure differences between coarse and fine texture. It provides us with the information about the size of texture elements. Fine textures have smaller value of this property than the coarse ones. We can measure coarseness of the image by applying the following steps:

Step 1—Take the average at every pixel over neighborhoods whose sizes are the power of 2. The average over the neighborhood of size $2^k \times 2^k$ ($k=0,1,2,3,4,5$) at every pixel is:

$$A_k(x, y) = \sum_{i=x-2^{k-1}}^{x+2^{k-1}-1} \sum_{j=y-2^{k-1}}^{y+2^{k-1}-1} g(i, j) / 2^{2k} \quad \dots(5)$$

where $g(i, j)$ is the gray-level at (i, j) .

Step 2—For each pixel, calculate the differences between the not overlapping neighborhoods in horizontal and vertical directions, as shown below:

Horizontal

$$E_{k,h}(x, y) = |A_k(x + 2^{k-1}, y) - A_k(x - 2^{k-1}, y)|$$

Vertical

$$E_{k,v}(x, y) = |A_k(x, y + 2^{k-1}) - A_k(x, y - 2^{k-1})| \dots(6)$$

Step 3—For each pixel, select the best size which gives the highest output value, as shown below:

$$S_{best}(x, y) = 2^k + 1 \quad \dots(7)$$

where k maximizes E in either direction

$$E_k(x, y) = \max[E_{k,h}(x, y), E_{k,v}(x, y)] \quad \dots(8)$$

Step 4—Take the average of S_{best} over the picture to be the coarseness measure F_{crs} , as shown below:

$$F_{crs} = \sum_{i=1}^m \sum_{j=1}^n S_{best}(i, j) / m * n \quad \dots(9)$$

where m and n are the effective size of the image.

Contrast

Contrast of the image is influenced by dynamic range of gray-levels in the image, polarization of the distribution of the black and white, sharpness of edges and period of repeating patterns. It could also stands for picture quality in the narrow sence. We can calculate contrast F_{con} as follows:

$$F_{con} = \sigma / (a_4)^n \quad \dots(10)$$

where $a_4 = \mu_4 / \delta_4$, μ_4 , the fourth moments; and δ^2 , the variance. Experimentally, $n=1/4$ was the best value obtained by Tamura *et al.*⁷.

Directionality

Directionality measures not the orientation itself but the presence of it in the image. It describes globally how the texture in the image is distributed or concentrated along certain orientations. If two images differ only in the orientation, the degree of this property will be the same for them. Following steps are used to measure directionality:

Step 1—For each point we calculate the modulus ΔG and local edge direction θ with the formula:

$$\begin{aligned}
 |\Delta G| &= (|\Delta_H| + |\Delta_V|) / 2 \\
 \theta &= \tan^{-1}(\Delta_V / \Delta_H) + \pi / 2
 \end{aligned} \quad \dots(11)$$

where Δ_H and Δ_V are the horizontal and vertical elements, calculated as the convolution of the image with the following 3×3 operators :

$$\begin{array}{ccc|ccc}
 -1 & 0 & 1 & 1 & 1 & 1 \\
 -1 & 0 & 1 & 0 & 0 & 0 \\
 -1 & 0 & 1 & -1 & -1 & -1
 \end{array} \quad \dots(12)$$

Step 2 —By count all pixels with $\Delta_G = t$ and quantizing θ by $(2k - 1)\pi / 2n \leq \theta \leq (2k + 1)\pi / 2n$,

we obtain the number of the points $N_\theta(k)$ which satisfy the above constraints. Then, building the edge probabilities histogram HD , as shown below:

$$HD(k) = N_\theta(k) / \sum_{i=0}^{n-1} N_\theta(i), \quad k = 0, 1, \dots, n-1 \quad \dots(13)$$

In our experiments, we used $n=36$ and $t=12$. The histogram curve for obvious directional image will exhibit a peak, for images without obvious direction it is relatively flat.

Step 3—Finally, the overall direction can be obtained by calculating the histogram peak sharpness, This measure can be defined as follows:

$$F_{dir} = \sum_p^{np} \sum_{\phi \in W_p} (\phi - \phi_p)^2 H_D(\phi) \quad \dots(14)$$

where p is the peak value of histogram; np , all the peak values of the histogram. For each p , W_p represents all the bins which include it, and p is the bin which has the highest peak value.

3 Results and Discussion

3.1 Relationship between Pattern features and Tie-dye Technique

ANOVA is a practical and valid statistics method which is used to calculate the significance of relevant factors on the experiment results. The tie-dye experiments in this paper have two factors which can pose joint impact upon results. To validate the significance of interaction upon the image data, we made two tests for each combination of the two factors.

In the first test, the rotation speed and the concentration are changing, and the rotation speed has three levels namely: 5 circles/min, 15 circles/min, and 30 circles/min. The concentration has five levels (Table 1). Each set of test data comprises 7 values including the average value of HSV tri-component of the valid tie-dye area and the proportion of tie-dye white area and three Tamura features (Table 2). Assuming that the pattern features are dependent, and the rotation speed and concentration are fixed with the confidence limit being 95%, we obtained the ANOVA (Table 3), according to the multi-variable analysis with SPSS software.

Table 1—Dyeing details [100g fabric]

Dye con. level	Concentration, g/L			
	Reactive black KN-B	Reactive red B-2BF	SSA	SA
1	0.45	0.05	20	10
2	0.9	0.1	30	15
3	2.7	0.3	40	20
4	5.4	0.6	50	25
5	10.8	1.2	60	30

Con.— Concentration.

According to the result of variance test (Table 3), the significance of rotation speed upon all features is smaller than 0.05. It represents the statistics implication that the rotation speed has great influence on all the features. Besides F_{crs} and F_{con} , the concentration has great influence on the other features. The significance of the cross impact of rotation speed and concentration upon H and V average-value and F_{con} and F_{dir} component is smaller than 0.05 as well, which means that it has impacts on them. However, the impact on S average value and Q and F_{crs} exceeds 0.05, which means it has no influence on them.

According to the result of overall test analysis (Tables 2 and 3), when the concentration is fixed, the influence of rotation speed on the color is obvious. The faster the rotation speeds, the deeper is the color. When the rotation is fixed, the influence of concentration on color is also obvious the higher the concentration the more obvious is the color impact. When the concentration becomes higher, the impact of rotation speed on color becomes lower. The lower the concentration, the more obvious is the impact of rotation speed on color. The higher the concentration, the less obvious is the impact of rotation speed on color. Under the same concentration, the slower the rotation speed, the larger is the white area. Under the same concentration, the impact of rotation speed of 30 circles/min and rotation speed of 15 circles/min on white area and color depth is not obvious. In case of the limited change in concentration, not only the color impact of low concentration & high rotation speed but also the high concentration & low rotation speed are not obvious. Under different concentrations, coloring effect is better with the rotation speed of 15 circles/min.

Table 3 shows that the former four features are similar under same experiment condition, but parts of texture features have some differences, such as No. 9, 10, 13, 15, and we can also see that their images are diverse. On the basis of experience, it can be said that production process can cause this uncertainty rather than texture features. So, as compared to color, texture features should be more effective to explain pattern. The Tamura coarseness is very consistent with image thickness according to visual perception, that is obviously rough texture image at lower concentration, its coarseness values to be significantly larger, relatively very fine texture the coarseness value of the image is significantly

Table 2 —Feature values for rotation speed and concentration dual-factor repeated test variance analysis

No.	Concentration	Speed	H _m	S _m	V _m	Q	F _{crs}	F _{con}	F _{dir}
1	1	1	0.5410	0.0778	0.9675	0.8843	0.4552	0.1171	0.2803
			0.5429	0.0663	0.9716	0.9007	0.4320	0.1000	0.3725
2	1	2	0.5424	0.1474	0.9373	0.8002	1.0000	0.2581	0.4181
			0.5450	0.1778	0.9236	0.7519	0.5565	0.3200	0.3036
3	1	3	0.5478	0.1355	0.9388	0.7931	0.6966	0.3202	0.7622
			0.5482	0.2641	0.8834	0.6685	0.7315	0.3318	0.9620
4	2	1	0.5483	0.1004	0.9542	0.8536	0.6995	0.2355	0.1199
			0.5486	0.1007	0.9543	0.8491	0.3891	0.2304	0.1129
5	2	2	0.5524	0.1861	0.9086	0.7519	0.5259	0.4152	0.4578
			0.5568	0.1613	0.9163	0.7643	0.7410	0.4748	0.5325
6	2	3	0.5549	0.2932	0.8524	0.6092	0.8138	0.4834	0.4628
			0.5541	0.2596	0.8700	0.6460	0.6150	0.4966	0.6293
7	3	1	0.5587	0.1575	0.9079	0.7717	0.4203	0.5368	0.1000
			0.5592	0.1940	0.8873	0.7236	0.5053	0.6054	0.1804
8	3	2	0.5626	0.2064	0.8702	0.7050	0.4840	0.7067	0.5144
			0.5692	0.2343	0.8558	0.6785	0.7070	0.7275	0.5135
9	3	3	0.5615	0.3334	0.8020	0.5747	0.7591	0.6494	0.9167
			0.5656	0.3450	0.7856	0.5287	0.2952	0.6871	0.7841
10	4	1	0.5672	0.2853	0.8167	0.6138	0.6151	0.7925	0.2425
			0.5622	0.1422	0.9136	0.8035	0.7514	0.5068	0.3833
11	4	2	0.5760	0.4036	0.6959	0.4539	0.4088	0.7748	0.6148
			0.5727	0.3575	0.7402	0.5171	0.3216	0.8784	0.6168
12	4	3	0.5750	0.3836	0.7163	0.4970	0.5644	0.8687	0.5236
			0.5744	0.3679	0.7353	0.5132	0.5458	0.8531	0.7149
13	5	1	0.5739	0.3314	0.7520	0.5547	0.3959	0.9764	0.3143
			0.5744	0.3233	0.7527	0.5711	0.6365	1.0000	0.4621
14	5	2	0.5904	0.4686	0.5624	0.3442	0.1275	0.6584	0.7801
			0.5934	0.4684	0.5654	0.3416	0.1000	0.6915	0.9222
15	5	3	0.6014	0.5130	0.4858	0.2998	0.1357	0.3992	0.9012
			0.5922	0.4635	0.5746	0.3719	0.2132	0.7216	1.0000

Table 3—Effect between subjects

Dual factor	H _m	S _m	V _m	Q	F _{crs}	F _{con}	F _{dir}
Speed	0.000	0.000	0.000	0.000	0.006	0.000	0.000
Concentration	0.000	0.000	0.000	0.000	0.835	0.098	0.000
Speed × concentration	0.006	0.356	0.009	0.191	0.079	0.001	0.008

Speed × concentration means interaction effect on the test results.

smaller. The influence of concentration on contrast is obvious; there is positive correlation between them. The influence of speed on contrast and directionality is obvious; there is positive correlation between them. In exceptional cases, there has been excessive staining in highest concentration process, so contrast disorders.

3.2 Forecast of Dyeing Production Technique Data

We found that the ANOVA results between two technical parameters and pattern features, can be used

to study the characteristic index of the tie-dye effect of different technical parameters. We made use of the regular pattern to establish the mathematical model to forecast the tie-dye parameters.

Artificial neural network (ANN) is the simplest abstraction and simulation to human brain. As a mathematic model, it offers a very strong solution to the studies of the functions of real number, discrete value or vector quantity from the sample. It can be used for the forecast of technical parameters used in this study.

Table 4—Correlation matrix of pattern features

Source	H _m	S _m	V _m	Q	F _{crs}	F _{con}	F _{dir}
F _{dir}	0.535**	0.694**	-0.642**	-0.686**	-0.274	0.240	1
F _{con}	0.669**	0.664**	-0.575**	-0.653**	0.224	1	
F _{crs}	-0.654**	-0.549**	0.670**	0.586**	1		
Q	-0.921**	-0.997**	0.973**	1			
V _m	-0.962**	-0.963**	1				
S _m	0.906**	1					

** p<0.01.

3.2.1 Neural Network Structure

This study uses the back propagation (BP) neural network model. It is the most widely-applied neural network model, and achieves the outstanding success in the model recognition area. To remove data redundancy of features, we did a correlation analysis on pattern features (Table 4). It is found that H_m, S_m, V_m and Q have strong correlation. Given that saturation is the key factor influencing the image pattern, we knock out H_m, V_m and Q from pattern features.

3.2.2 Learning Algorithm

There are 4 BP network input units, including S_m, F_{crs}, F_{con}, F_{dir}, and 1 output unit. Value ranges between 1 and 15, which represents the cross combination number of rotation speed and concentration in the variance test. The number of hidden network layer is 1. According to Kolmogorov theory, assuming the number of hidden network layer as 2×4+1, we used *transig* as the transition function from input layer to hidden layer, *purelin* as the transition function from hidden layer to output layer, and L-M optimization algorithm.

3.2.3 Result Analysis

Take 30 sets of data (Table 2) as the training sample, the best error tolerance as 0.001 and the training algebra as 5000. Figure 4 shows the 16th training results, the training contraction is very fast, and the best tolerance is achieved with 2977 times. Figure 5 shows training forecast results, where R value is 0.99997; R value reaching 1 means good network forecast effect. Ordinate is network output value, where empty circle dot is the output, and each value is very close to its target tolerance. The use of the training sample as test data can achieve the forecast accuracy rate of 100%. In contrast, the other 15 trainings fail to reach the best tolerance within the training algebra of 5000.

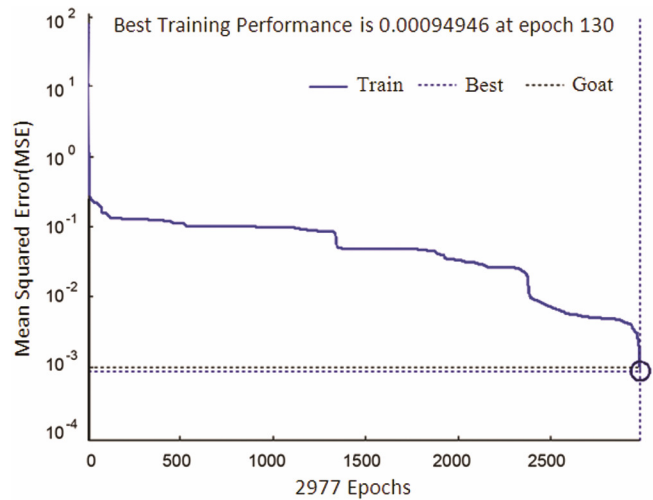


Fig. 4—BP training error indicators decline curve

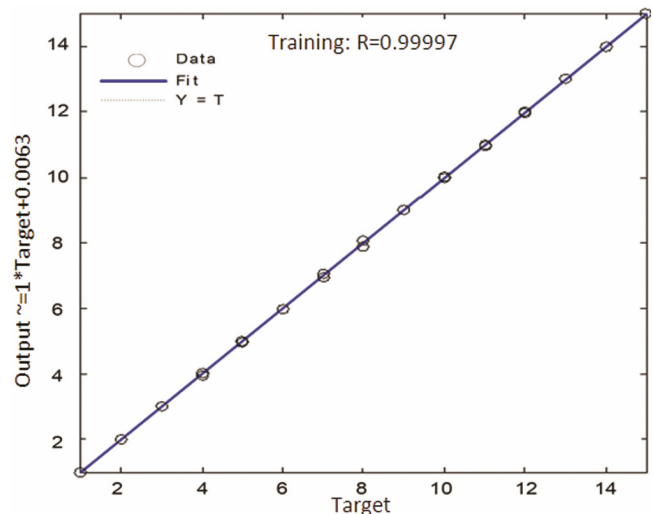


Fig. 5—BP training prediction map

In order to better validate the network forecast effect, we made 15 more tests. The forecast accuracy rate also reached 100%. Figure 6 indicates the effect, where (+) is the test sample and the (o) is the target point.

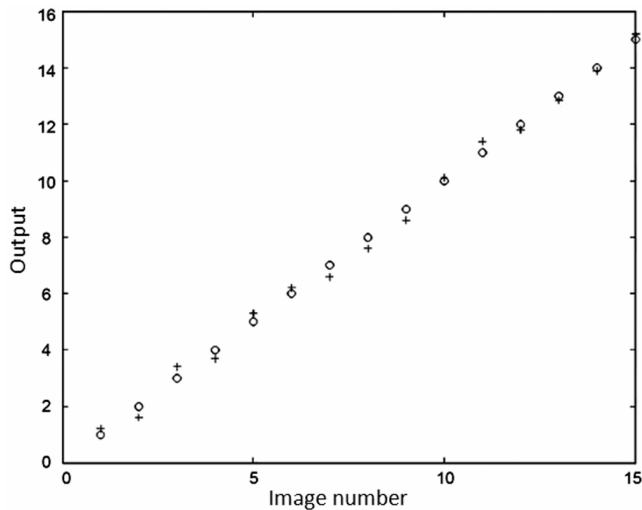


Fig. 6—BP test results figure

4 Conclusion

This study extracts the average value of HSV tri-component of the valid tie-dye area and the proportion of tie-dye white area in the HSV color space and Tamura features as a quantitative measure for evaluating the pattern of tie-dye image. The rotation speed and concentration dual-factor repeated tests are designed for analyzing and validating the impact of concentration and rotation speed on the color and texture of tie-dye pattern. The results have proved that the rotation speed has great influence on all the image features; besides F_{crs} and F_{con} , the concentration has great influence on the other features. In the features, it is found that H_m , S_m , V_m and Q have strong correlation through correlation analysis. So, we used S_m , F_{crs} , F_{con} and F_{dir}

for technique forecast. We designed the BP neural network to forecast the tie-dye concentration and rotation speed with pattern features. The training and forecast success rate reaches 100%. The result demonstrates that the set of index can effectively predict the tie-dye technique.

Acknowledgement

Authors thankfully acknowledge the funding support by National-sponsored Social Sciences (No.12BMZ049), the Ministry of Education for New Century Excellent Talents Project of China (No. NCET-10-0454), and Jiangsu Natural & Social Science Foundation (No.BK2012363, No.BY2015012-01).

References

- Huang Xiao-hua, Wang Chunmao & Zheng Wen-ming, *J Image Graphics*, 15(3) (2010) 422.
- Shang Ke-ke, Liu Ying & Lu Yi-xing, *J Optoelectronics Laser*, 18(11) (2007) 1391.
- Hsu R-L, Abdel-Mottaleb M. & Jain A K., *IEEE Trans Pattern Analysis Machine Intelligence*, 24(5) (2002) 696.
- Amine A, Ghouzali S & Rziza M, *IEEE Tr PAMI*, 24 (2002) 696.
- Li Wei & Li De-ren, *J Image Graphics*, 16(9) (2011) 1691.
- Martel-Brisson N & Zaccarin A, *IEEE Trans Pattern Anal Mach Intell*, 29(7) (2007) 1133-1146.
- Cucchiara R, Grana C & Piccardi M, *IEEE Trans Pattern Anal Mach Intell*, 25 (10) (2003) 1337.
- Yang Hong-ying, Wu Ju-neng, Yu Yong-jian & Wang Xiang-yang, *J Image Graphics*, 13(10) (2008) 2035.
- Liu Y, Zhang D, Lu G & Ma W Y, *Pattern Recogn*, 40 (2008) 262.
- Tamura H, Mori S & Yamawaki T, *IEEE Trans Systems Man Cyber*, 8(6) (1978) 460.
- Otsu N, *IEEE Trans Syst Man Cybern*, 9 (1979) 62.